Journal of the Korean Ceramic Society
Vol. 56, No. 1, pp. 49–55, 2019.

https://doi.org/10.4191/kcers.2019.56.1.08

Hardness and Oxidation Resistance of $Ti_{0.33}Al_{0.67}N$/CrN Nano-multilayered Superlattice Coatings

Seung-Su Ahn*, Kyung-Sik Oh, Tai-Joo Chung**†, and Jong-Keuk Park*****

**Production Engineering Research Center, KORLOY, Cheongju 28589, Korea*

***School of Advanced Materials Engineering, Industrial Technology Center for Environment-friendly Materials, Andong National University, Andong 36729, Korea*

****Center for Electronic Materials, Korea Institute of Science and Technology, Seoul 02792, Korea*

(Received September 6, 2018; Revised December 18, 2018; Accepted December 19, 2018)

ABSTRACT

$Ti_{0.33}Al_{0.67}N$/CrN nano-multilayers, which are known to have excellent wear resistance, were prepared using an unbalanced magnetron sputter to have various periods of 2–5 nm. $Ti_{0.33}Al_{0.67}N$ had a hexagonal structure in a single layer, but converted to a cubic structure by forming a multilayer with CrN, which has a cubic structure. Thus, $Ti_{0.33}Al_{0.67}N$ formed a superlattice in the multilayer. The $Ti_{0.33}Al_{0.67}$/CrN multilayer with a period of 2.5 nm greatly exceeded the hardness of the $Ti_{0.33}Al_{0.67}N$ and the CrN single layer, reaching 39 GPa. According to the low angle X-ray diffraction results, the $Ti_{0.33}Al_{0.67}N$/CrN multilayer maintained its as-coated structure to a temperature as high as 700°C and exhibited hardness of 30 GPa. The thickness of the oxide layer of the $Ti_{0.33}Al_{0.67}N$/CrN multilayered coating was less than one-tenth of those of the single layers. Thus, $Ti_{0.33}Al_{0.67}N$/CrN multilayered coating had hardness and oxidation resistance far superior to those of its constituent single layers.

Key words : $Ti_{0.33}Al_{0.67}N$, CrN, Multilayer, Hardness, Oxidation resistance

1. Introduction

Cutting tools play a critical role in the mass manufacturing of structural materials. With an increasing variety and strength of workpiece materials, enhanced mechanical and thermal properties are in demand for cutting tool materials. In response to this demand, cutting performance has been increased by coating the cutting tool surface with a layer of materials with outstanding properties. Among such materials, nano-multilayer coating was reported to exhibit high hardness and wear resistance, such that the material is described as "superhard"; the material was found to critically improve cutting performance.[1] The nano-multilayer coating is composed of two types of materials that are coated with nanometer thickness in alternating order; coating is typically comprised of a high hardness material and low hardness material.[1] The performance of nano-multilayer coatings is determined by the selected materials and the period or repetition interval of the coating layer.[2]

A single layer of the multilayer coating is very thin, with a thickness of only a few nm; phenomena different from those observed for a single coating are observed. For example, when the single layer of a multilayer coating has a different crystal structure from that of a single coating, it is called a superlattice.[1] The superlattice is the result of the atomic arrangement of adjacent layers when layering the atoms in the multilayer coating. Compared to materials in equilibrium state, the superlattice layer has a different structure and lattice constant, so stress is developed accordingly. This stress is understood as one of the reasons that the multilayer structure coating exhibits high hardness.[3-5]

This "superhard" performance was first discovered with the TiN and VN combination, which was reported to have a hardness exceeding 50 GPa.[1] Also, CrN and AlN is a representative combination with high hardness.[6] While CrN and VN play the roles of somewhat soft material, TiN and AlN play the roles of high hardness material. The $Ti_{1-x}Al_xN$, alloy of TiN and AlN, was reported to have outstanding properties as a cutting tool material,[7,8] as well as excellent thermal stability and oxidation resistance.[9,10]

Thermal stability is required because a nano-multilayer coating is exposed to severe frictional heat during high speed cutting, similar to other cutting tool materials. For example, while a cutting tool of a diamond structure has outstanding hardness, the tool is not thermally stable, so there are limitations to its application.[11] Oxidation resistance is also required for the nano-multilayer coating as the hardness can only be maintained when the multilayer structure was not broken up by diffusion. The breakup of the multilayer structure signifies the breakup of the superlattice state, which can lead to degradation of the excellent hardness.[2] In other words, a multilayer structure refers to a clear separation of the composition between layers according to components. When the temperature increases, inter-

†Corresponding author : Tai-Joo Chung
E-mail : tjchung@anu.ac.kr
Tel : +82-54-820-5886 Fax : +82-54-820-6211

diffusion leads to the disappearance of component boundaries and the multilayer structure becomes meaningless. Additionally, when material is exposed to high temperatures during cutting, oxidation can occur from the reaction with oxygen in the air. The cutting performance cannot be maintained or the oxidized parts separate from the base material as particles in oxide state.

Therefore, the objective of this study was to fabricate and investigate the properties of nano-multilayer coating with various periods for the $Ti_{0.33}Al_{0.67}N$ component corresponding to the Al in $Ti_{1-x}Al_xN$ being 0.67, and CrN. In order to apply the nano-multilayer coating, sputtering at two targets has to be carried out alternatively using sputtering equipment that supports two targets, so this study used an unbalanced magnetron for sputtering.[12] Compared to regular equipment, unbalanced magnetron sputtering equipment effectively produces plasma for the coating, and a jig that simultaneously undergoes revolution and rotation was manufactured for convenient control of the double layer period according to the revolution and rotation speeds. Also, this study aimed to observe the heat treatment stability and oxidation properties of the $Ti_{0.33}Al_{0.67}N$/CrN multilayer coating with various periods and investigate the effect of the nano-multilayer structure.

2. Experimental Procedure

2.1. Deposition

The unbalanced magnetron sputtering equipment shown in Fig. 1 was used to deposit the multilayer coating. As shown in the figure, targets were located on the left and the right. The substrate was fixed to the jig, which simultaneously carried out revolution and rotation so that deposition occurred alternately from each target to fabricate a multilayer coating with two components alternately deposited. The targets used for the deposition had dimensions of 12.8 cm × 30 cm. One target used $Ti_{0.33}Al_{0.67}$ and the other target used Cr, while a Si (100) wafer was used as the substrate. A distance of 70 mm between the target and substrate, chamber pressure of 3×10^{-5} torr, and deposition temperature of 400°C were maintained during deposition.

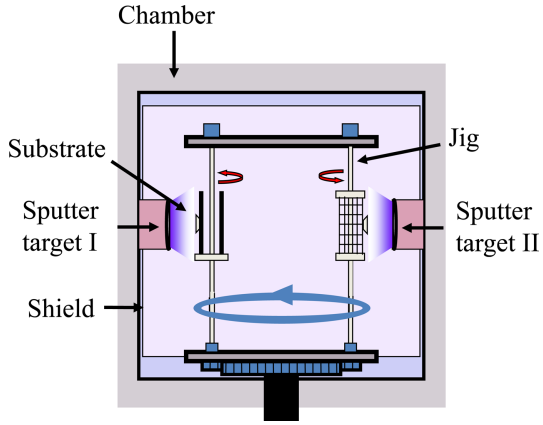

Fig. 1. Schematic illustration of unbalanced magnetron sputtering device used for preparation of multilayered films.

Prior to the deposition, to carry out substrate cleaning using Ar plasma, a bias voltage of –800 V was maintained on the substrate for 10 minutes. During deposition, the bias was set to –120 V and the Cr buffer layer was deposited first, followed by the CrN layer on top. Then, a multilayer coating was obtained by alternating $Ti_{0.33}Al_{0.67}N$ and CrN. The ratio of the reacting gases Ar and N_2 was 2:3 and the total flow rate was 50 sccm. The deposition time was adjusted to 2–3 h so that the total coating thickness was 2–3 μm. The rotation speed of the substrate holder was varied to control the thickness of the $Ti_{0.33}Al_{0.67}N$/CrN pair layer in the multilayer coating.

2.2. Structural Analysis

Low angle X-ray diffraction (M03XHF22 MAC Science) was used to measure the period of the multilayer coating and high angle X-ray diffraction (M03XHF22 MAC Science) was used to analyze the crystal structure. A modification of Bragg's Law shown in Eq. (1) was used to determine the period (Λ).[13] Here, n is the Bragg peak index, θ is the n-th Bragg peak diffraction angle, and δ is the real component of the average index of the superlattice refraction. The period was calculated from the slope of the line obtained through the relationship between $\sin^2\delta$ and n^2.

$$\sin^2\theta = \left(\frac{n\lambda}{2\Lambda}\right)^2 + 2\delta \quad (1)$$

The (220) peak was used to determine the lattice constant from the high angle X-ray diffraction.[14]

2.3. Property Evaluation

A nanoindenter (XP MTS) was used to measure the hardness of the multilayer and a ball-on-disc type tribometer, fabricated in-house, was used to measure the wear resistance and friction coefficient.

2.4. Thermal Stability

A rapid thermal annealing device was used to evaluate the high temperature stability of the multilayer through 1 h of heat treatment at 600–800°C under an Ar atmosphere. After heat treatment, analysis was carried out using low angle X-ray diffraction to determine the presence of remaining multilayers. Also, the nanoindenter was used after the heat treatment to measure the hardness and observe the hardness variation according to the multilayer state.

In order to evaluate the oxidation resistance, heat treatment was conducted at 700–800°C and high angle X-ray diffraction was used to determine the production of oxides. To evaluate the oxidation layer thickness, Auger electron spectroscopy (model 670 PHI) was used to observe the composition variation in the coating depth direction. It was found that the oxygen content decreased and the nitrogen content increased in the depth direction, and the depth at which the

oxygen and nitrogen concentrations were equal was measured as the oxidation layer thickness. A scanning electron microscope (SEM, s-4200 Hitachi) was used to observe the heat treated microstructure.

2.5. Stress Evaluation

In order to assess the single layer and multilayer stress (σ), the coating was deposited on a Si strip of 2 mm width, 40 mm length, and 100 μm thickness; the curvature radius (κ) was measured using in-situ stress measurement equipment (JIL Tech) and the residual stress was calculated by applying the Stoney formula shown in Eq. (2).[15] Here, E is the Young's modulus of Si, ν is the Poisson's ratio of Si, and h_s and h_f are the substrate thickness and measured coating thickness, obtained using SEM.

$$\sigma = \frac{Eh_s^2\kappa}{6h_f(1-\nu)} \quad (2)$$

3. Results and Discussion

Figure 2 shows the high angle X-ray diffraction pattern obtained after the single layer depositions of $Ti_{0.33}Al_{0.67}N$

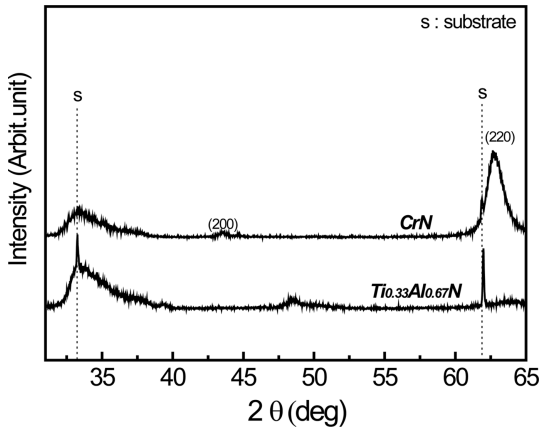

Fig. 2. High angle X-ray diffraction patterns of $Ti_{0.33}Al_{0.67}N$ and CrN single layered films.

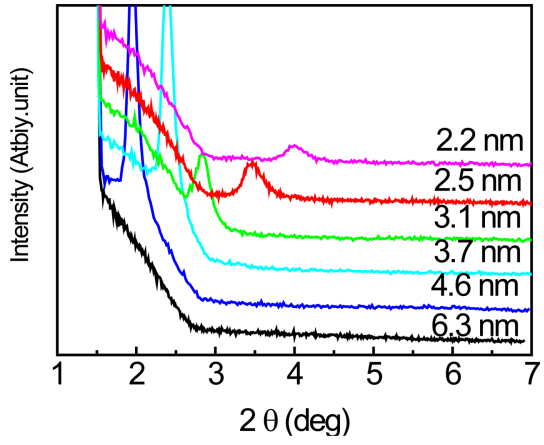

Fig. 3. Low angle X-ray diffraction patterns of $Ti_{0.33}Al_{0.67}N$/CrN multilayer.

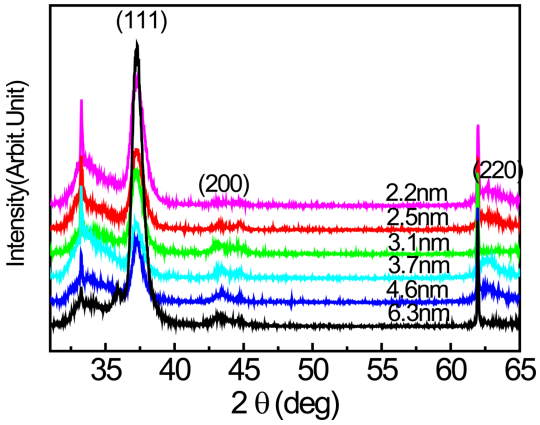

Fig. 4. High angle X-ray diffraction patterns from $Ti_{0.33}Al_{0.67}N$/CrN multilayers with various bilayer periods.

and CrN. CrN is the cubic phase of the NaCl crystal structure and $Ti_{0.33}Al_{0.67}N$ is the hexagonal phase of the Wurzite structure. Fig. 3 shows the low angle X-ray diffraction pattern after fabricating $Ti_{0.33}Al_{0.67}N$ and CrN into multilayers. Fig. 3 shows that the peak locations (2θ) were different; this was applied to Eq. (1) to calculate the period, which is shown in the figure. The increase in peak intensity in Fig. 3 suggests the clear interface of multilayer and distinct boundary.[13] Also, when the period is small, the peak strength was relatively low, with a broadening of width. Fig. 4 shows the high angle X-ray diffraction pattern obtained after fabricating $Ti_{0.33}Al_{0.67}N$ and CrN into multilayers. It was found that $Ti_{0.33}Al_{0.67}N$ also had a cubic structure for all periods when in multilayer form. From Figs. 2–4, it was determined that $Ti_{0.33}Al_{0.67}N$ with a hexagonal structure in single layer form had a cubic structure when fabricated together with CrN.

This phenomenon in which $Ti_{0.33}Al_{0.67}N$ takes on the structure of the base material rather than its original crystal structure is called a superlattice.[1] This is a result of the $Ti_{0.33}Al_{0.67}N$ taking on the atomic arrangement of CrN during the deposition process and, because the original stable structure and lattice constant are no longer taken on. Since the surplus free energy increases as the $Ti_{0.33}Al_{0.67}N$ layer becomes thicker, resulting in increased instability, it can be considered that this is a condition that is only observed for thin films of nanometer scale, as used in this study.

Figure 5 shows the $Ti_{0.33}Al_{0.67}N$/CrN multilayer hardness according to the period. The hardness measurement results for the $Ti_{0.33}Al_{0.67}N$ and CrN single layers were approximately 25 and 29 GPa, respectively. The hardness for the nano-multilayer was significantly greater than that of the single layers. This increase varied according to the period, where the maximum hardness of 39 GPa was obtained for the period of 2.5 nm. Since the hardness of the nano-multilayer was always greater than the average of the hardnesses of the two materials calculated through the rule of mixture, it was determined that there was a mechanism

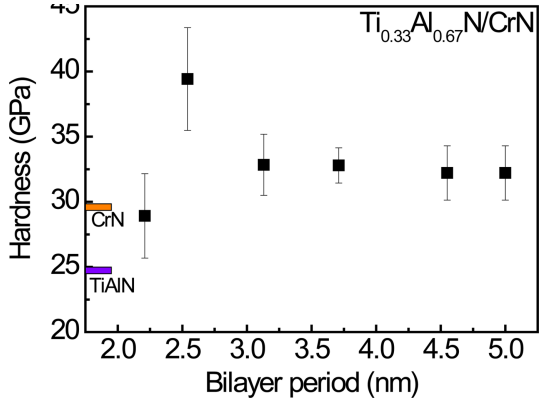

Fig. 5. Variation of hardness in $Ti_{0.33}Al_{0.67}N$/CrN multilayers with respect to periods of bilayers.

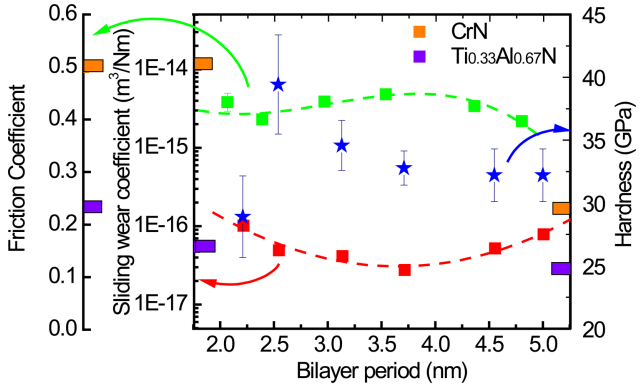

Fig. 6. Variation of sliding wear coefficient, friction coefficient, and hardness in $Ti_{0.33}Al_{0.67}N$/CrN multilayers with respect to periods of bilayers.

that enhanced the hardness when forming the nano-multilayer. Fig. 6 shows the wear resistance, hardness, and friction coefficient relationship for the nano-multilayer according to the period. For almost all periods, the sliding wear coefficient, which represents the wear resistance property of the nano-multilayer, was lower than the value corresponding to the mixture rule of the single layer. Depending on the period, the lowest value was obtained for 3–4 nm and the value tended to increase at higher periods. On the other hand, the friction coefficient showed relatively smaller variation according to the period and the friction coefficient lay within the mixture rule range with the friction coefficients of the single layers on either end. Thus, it was determined that the effect of the friction coefficient on the wear resistance property was relatively small.

From the above results, it was found that unbalanced magnetron sputtering can be used to effectively fabricate a $Ti_{0.33}Al_{0.67}N$ /CrN nano-multilayer by controlling the period to 2–5 nm. The $Ti_{0.33}Al_{0.67}N$ in the nano-multilayer was observed to be of cubic structure, a superlattice, resulting in a significant increase in the hardness of the nano-multilayer compared to that of the single layer, along with enhanced wear resistance.

Since actual cutting tools are exposed to severely high

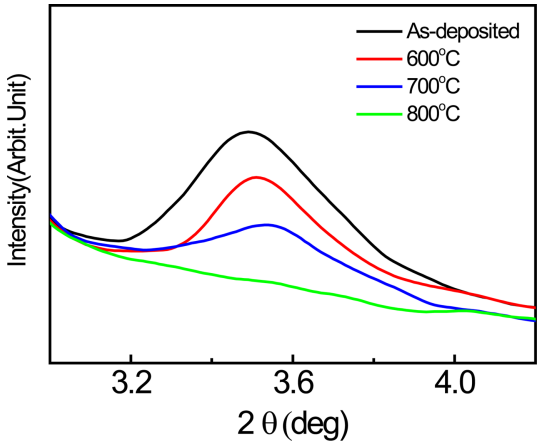

Fig. 7. Low angle X-ray diffraction patterns of as-deposited $Ti_{0.33}Al_{0.67}N$/CrN multilayer coatings and coatings heat treated at 600°C, 700°C, and 800°C for 1 h.

temperatures due to the high speed of cutting, changes after heat treatment were observed. Fig. 7 shows low angle X-ray diffraction observation results after heat treatment at 600–800°C under Ar atmosphere for the nano-multilayer. It was observed that the peak strength decreased as the heat treatment temperature increased. The peak strength in the low angle X-ray diffraction is related to the clearness of the interface and the slope of the composition. When the composition slope is gradual and the interface is not clear, the peak strength weakens. Increases in heat treatment temperature induce intermixing by diffusion at the interface, resulting in composition slope becoming gradual. Eventually, interdiffusion at the interface causes the peak strength to decrease.[13] As shown in Fig. 7, the peak weakened as the heat treatment temperature increased for the $Ti_{0.33}Al_{0.67}N$/CrN multilayer and, at 800°C, it was determined that the nano-multilayer structure had essentially broken up.

Figure 8 shows the variation of the post heat treatment hardness under an Ar atmosphere. While a multilayer that did not undergo heat treatment had a hardness of 40 GPa, heat treatment reduced the hardness to about 30 GPa. In addition to the degradation of the coating itself, there can be other factors that contribute to this change, including the

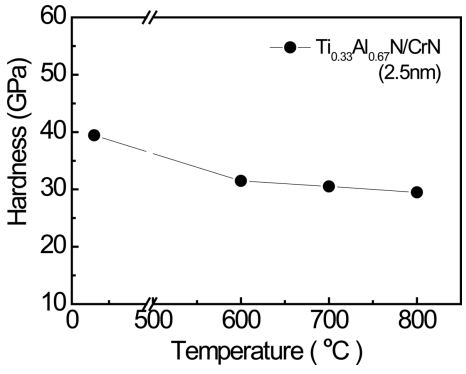

Fig. 8. Change of hardness of $Ti_{0.33}Al_{0.67}N$/CrN multilayer coatings with annealing high temperature.

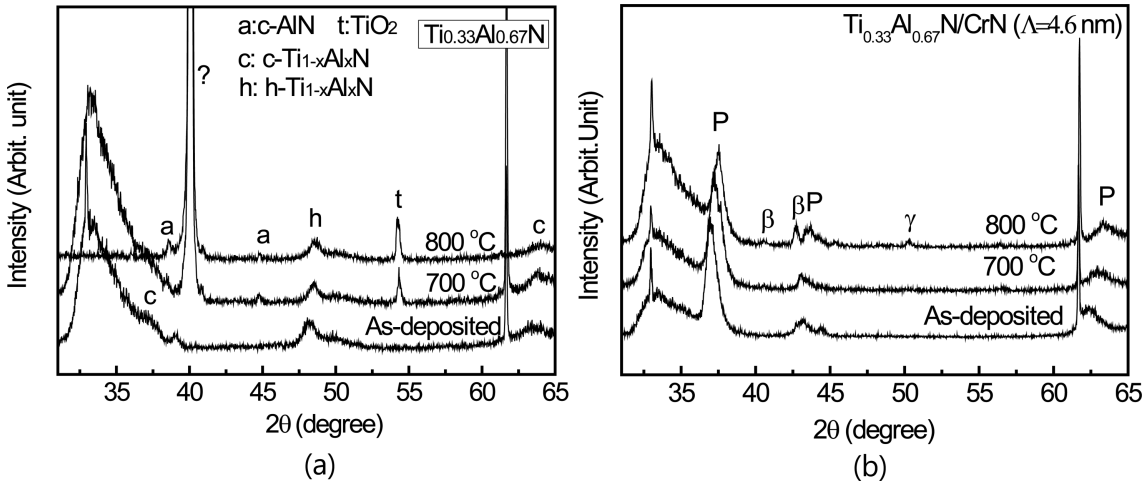

Fig. 9. High angle X-ray diffraction patterns from (a) $Ti_{0.33}Al_{0.67}N$ single layer coating and (b) $Ti_{0.33}Al_{0.67}N$/CrN multilayer coating after annealing in the air at various temperatures.

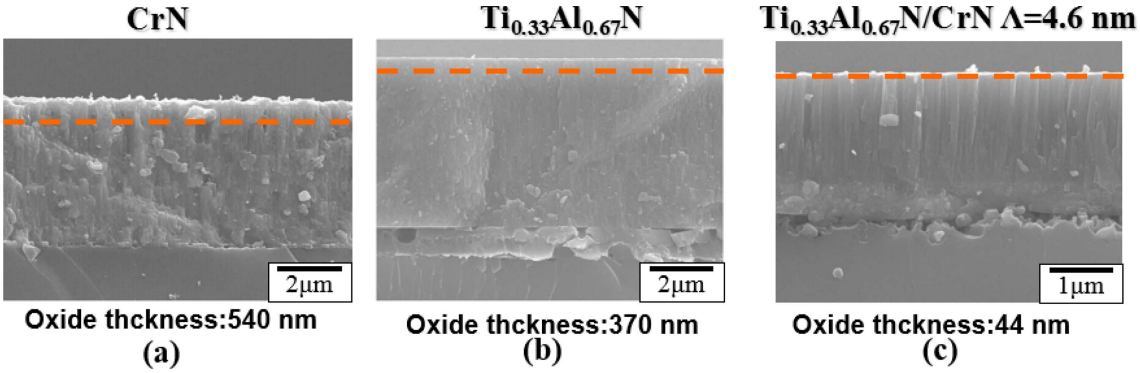

Fig. 10. Cross sections showing the coating and oxidation layers of (a) CrN, (b) $Ti_{0.33}Al_{0.67}N$, and (c) $Ti_{0.33}Al_{0.67}N$/CrN multilayer after annealing in air at 800°C. The broken line indicates the boundary between oxidation and coating, determined by AES analysis.

separation of the film according to the thermal expansion mismatch and reduction of the adhesion strength between the coating and the substrate.

When the cutting tool is exposed to high temperatures, loss of stability of the multilayer can occur, along with changes due to oxidation, as shown in Figs. 7 and 8. Fig. 9(a) shows high angle X-ray diffraction pattern results for the $Ti_{0.33}Al_{0.67}N$ single layer after heat treatment at 700°C and 800°C under air. In the case of the $Ti_{0.33}Al_{0.67}N$ single layer, heat treatment at 700°C resulted in the appearance of a TiO_2 oxide peak(t). Fig. 9(b) shows the high angle X-ray diffraction pattern observed for the nano-multilayer after heat treatment under air. Here, Cr_2O_3 began to appear weakly at 800°C; this is considered the result of oxidation of Cr in the buffer layer, caused by the partial separation of the film during heat treatment due to the thermal expansion coefficient difference. Comparison between Figs. 9(a) and (b) reveals that when a nano-multilayer is formed, the oxidation onset temperature increased because TiO_2 did not appear, unlike the case of the single layer. Auger electron microscropy (AES) was used to measure the thickness of oxidation layer because accurate observation is difficult due to the partial separation of the film during oxidation.

Figure 10 shows the oxidation layer thickness observation results for the single layer and nano-multilayer. AES was used to observe the oxygen and nitrogen concentrations

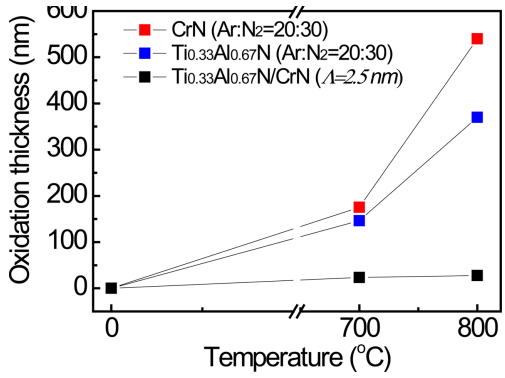

Fig. 11. Thickness of oxidation layer of CrN, $Ti_{0.33}Al_{0.67}N$, and $Ti_{0.33}Al_{0.67}N$/CrN multilayer after annealing in air at 700°C and 800°C.

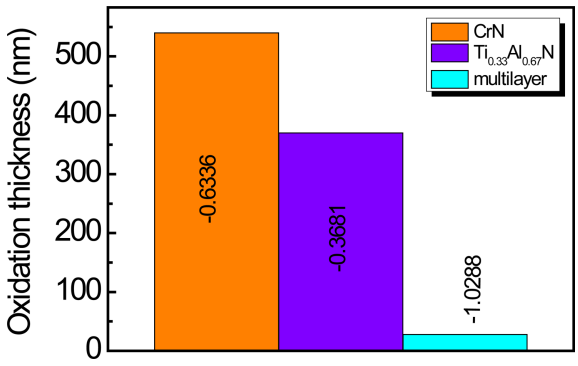

Fig. 12. Thickness of oxidation layer of CrN, $Ti_{0.33}Al_{0.67}N$, and $Ti_{0.33}Al_{0.67}N$/CrN multilayer after annealing in air at 800°C. The stress values (in GPa) before annealing are shown in the graph.

according to the depth. Fig. 10 shows the oxidation layer thickness, which was determined by the depth at which the oxygen and nitrogen concentrations were equal. The oxidation layer thickness increased along with the heat treatment temperature. The oxidation layer thicknesses were 540 nm for the CrN single layer heat treated at 800°C and 370 nm for the $Ti_{0.33}Al_{0.67}N$ single layer. On the other hand, the oxidation layer thickness for the nano-multilayer was only 44 nm when the period was 4.6 nm, so it was found that the oxidation resistance significantly increased. Fig. 11 shows the observation results for the oxidation layer thickness as determined in Fig. 10 for the heat treatment temperatures of 700°C and 800°C. The figure reveals the inhibition of oxidation in the nano-multilayer coatings.

Figure 12 shows the measurement of the residual stress developed to the single layer and nano-multilayer. The stress was calculated from the curvature radius observed after deposition on the 100 μm thickness Si strip.[15] For the single layer, $Ti_{0.33}Al_{0.67}N$ exhibited outstanding oxidation resistance compared to that of CrN due to the addition of Al. Meanwhile, in the case of the $Ti_{0.33}Al_{0.67}N$/CrN nano-multilayer obtained by repeatedly stacking nanometer scale thickness CrN and $Ti_{0.33}Al_{0.67}N$ single layers, a compressive stress of 1 GPa, which is greater than that of the single layer film, was accumulated; this stress is thought to contribute to the formation and the maintaining of a protective oxide layer that inhibits crack generation during oxidation. When the oxidation resistant component like Al is added, high oxidation resistance can only be expected while the protective layer is maintained without crack generation. In this study, the $Ti_{0.33}Al_{0.67}N$/CrN nano-multilayer was fabricated and it was found that compressive stress of about 1 GPa was accumulated; it was possible to maintain the adhesion with the base material because the layers were so thin that high oxidation resistance was possible from the formation of a stable protective oxide film. Further study on the mechanisms behind such oxidation resistance needs to be carried out for greater in-depth understanding.

4. Conclusions

A nano-multilayer coating composed of $Ti_{0.33}Al_{0.67}N$/CrN with various periods ranging between 2–5 nm was fabricated using unbalanced magnetron sputtering. The $Ti_{0.33}Al_{0.67}N$ exhibited a cubic structure in nano-multilayer form like that of CrN, so it was a superlattice with a crystal structure different from the single layer form. This superlattice formation resulted in the $Ti_{0.33}Al_{0.67}N$/CrN nano-multilayer having a hardness of 39 GPa when the period was 2.5 nm, which significantly exceeded the hardnesses of $Ti_{0.33}Al_{0.67}N$ and CrN. In order to evaluate the thermal stability of the $Ti_{0.33}Al_{0.67}N$/CrN coating during cutting, the coating was heated under an Ar atmosphere; the nano-multilayer structure dissipated at 800°C and the hardness decreased to 30 GPa. AES was used to measure the thickness of the oxidation layer produced when the nano-multilayer was heated in air. It was found that the thickness of the oxidation layer produced at the nano-multilayer was about 1/10 of the oxidation layer thicknesses for $Ti_{0.33}Al_{0.67}N$ and CrN, so the thermal stability and oxidation resistance had improved greatly. These hardness and oxidation resistance improvements of the nano-multilayer coating were determined to be due to the formation of superlattice in the nano-multilayer and the high residual compressive stress of about 1 GPa.

Acknowledgments

This work was supported by a grant from 2016 research funds of Andong National University. The authors would like to thank Korloy and the Korea Institute of Science and Technology (KIST) for helping with this study.

REFERENCES

1. J. S. Koehler, "Attempt to Design a Strong Solid," *Phys. Rev. B,* **2** [2] 547–50 (1970).
2. W. Herr, B. Matthes, E. Broszeit, M. Meyer, and R. Suchentrunk, "Influence of Substrate Material and Deposition Parameters on the Structure, Residual Stresses, Hardness and Adhesion of Sputtered CrxNy Hard Coatings," *Surf. Coat. Technol.,* **60** [1–3] 428–33 (1993).
3. J. W. Cahn, "Hardening by Spinodal Decomposition," *Acta Metall.*, **11** [12] 1275–82 (1963).
4. M. Kato, T. Mori, and L. H. Schwartz, "Hardening by Spinodal Modulated Structure," *Acta Metall.,* **28** [3] 285–90 (1980).
5. A. K. Head, "The Interaction of Dislocation and Boundaries," *Philos. Mag.,* **44** [348] 92–4 (1953).
6. J.-K. Park and Y.-J. Baik, "The Crystalline Structure, Hardness and Thermal Stability of AlN/CrN Superlattice Coating Prepared by D.C. Magnetron Sputtering," *Surf. Coat. Technol.,* **200** [5-6] 1519–23 (2005).
7. H. G Prengel, A. T. Santhanam, R. M. Penich, P. C. Jindal, and K. H. Wendt, "Advanced PVD-TiAlN Coatings on Carbide and Cermet Cutting Tools," *Surf. Coat. Technol.,* **94–95** [10] 597–602 (1997).

8. A. Raveh, M. Weiss, M. Pinkas, D. Z. Rosen, and G. Kimmel, "Graded Al–AlN, TiN, and TiAlN Multilayers Deposited by Radio-Frequency Reactive Magnetron Sputtering," *Surf. Coat. Technol.,* **114** [2–3] 269–77 (1999).
9. W. D. Münz, "Titanium Aluminum Nitride Films: A New Alternative to TiN Coatings," *J. Vac. Sci. Technol., A,* **4** [6] 2717–25 (1986).
10. O. Knotek and T. Leyendecker, "On the Structure of (TiAl)N-PVD Coatings," *J. Solid State Chem*., **70** [2] 318–22 (1987).
11. K. Holmberg, H. Ronkainen, and A. Mattews, "Tribology on Thin Coatings," *Ceram. Int.,* **26** [7] 787–95 (2000).
12. P. J. Kelly and R. D. Arnell, "Characterization Studies of the Structure of Al, Zr, and W Coatings Deposited by Closed-Field Unbalanced Magnetron Sputtering," *Surf. Coat. Technol.,* **97** [1–3] 595–602 (1997).
13. E. Fullerton, I. K. Schuller, H. Vanderstraeten, and Y. Bruynseraede, "Structural Refinement of Superlattice from X-Ray Diffraction," *Phys. Rev. B,* **45** [16] 9292–310 (1992).
14. A. Bendavid, P. J. Martin, X. Wang, M. Wittling, and T. J. Kinder, "Deposition and Modification of Titanium Nitride by Ion Assisted Arc Deposition," *J. Vac. Sci. Technol. A,* **13** [3] 1658–64 (1995).
15. X. Feng, Y. Huang, and A. J. Rosakis, "On the Stoney Formular for a Thin Film/Substrate System with Non-Uniform Substrate Thickness," *Trans. ASME*, **74** [6] 1276–81 (2007).